치의학박사 학위논문

Acoustic emission analysis of tooth-composite interfacial debonding during photo-cured composite restoration

광중합 복합레진 수복 중 복합레진-치아 계면의 접착 파괴에 관한 음향방출분석

2013 년 2 월

서울대학교 대학원

치의과학과 치과보존학 전공

조 낙 연

Abstract

Acoustic emission analysis of tooth-composite interfacial debonding during photo-cured composite restoration

Nak Yeon Cho, D.D.S., M.S.D.

Program in Conservative Dentistry,

Department of Dental Science,

Graduate School, Seoul National University

(Directed by Prof. In-Bog Lee, D.D.S., M.S.D., Ph.D.)

***Objectives*:** The aim of this study was to detect tooth-composite interfacial debonding during composite restoration by means of acoustic emission (AE) analysis, and to investigate the effect of composite properties, adhesives systems, and light curing methods on AE characteristics.

***Methods*:** The polymerization shrinkage, peak shrinkage rate, flexural modulus, and shrinkage stress of a methacrylate-based universal hybrid, a flowable, and a silorane-based composite were measured. Class I cavities on 49 extracted

premolars were restored with one of three composites and one of the following adhesives: two etch-and-rinse adhesives, two self-etch adhesives, and an adhesive for the silorane-based composite. An AE sensor was applied with grease to the glass slide holding the tooth to detect debonding sound at the tooth-composite interface. The signals from the AE sensor were amplified and stored on a computer. AE analysis was done for 2,000 sec during light-curing. SEM images of the tooth-composite interface were obtained with the epoxy replicas of sliced specimens.

***Results*:** The silorane-based composite exhibited the lowest shrinkage (rate), the longest time to peak shrinkage rate, the lowest shrinkage stress, and the fewest AE events. AE events were detected immediately after the beginning of light-curing in most composite-adhesive combinations, but not until 40 sec after light-curing began for the silorane-based composite. AE events were concentrated at the initial stage of curing in self-etch adhesives compared with etch-and-rinse adhesives. In the SEM image, flowable resin showed wider gaps at the dentin-composite interface compared with the other groups, while silorane-based composite showed narrower gaps.

***Significance*:** Reducing the shrinkage (rate) of composites resulted in reduced shrinkage stress and less debonding as evidenced by fewer AE events. AE is an effective technique for monitoring, in real time, the debonding kinetics at the

tooth-composite interface.

Keywords: acoustic emission, composite, interfacial debonding, polymerization shrinkage stress, silorane

Student number: 2011-30678

목 차

Acoustic emission analysis of tooth-composite interfacial debonding during photo-cured composite restoration

Nak Yeon Cho, D.D.S.,M.S.D.

Program in Conservative Dentistry,

Department of Dental Science,

Graduate School, Seoul National University

(Directed by Prof. In-Bog Lee, D.D.S., M.S.D., Ph.D.)

I. INTRODUCTION

Polymerization shrinkage accompanying the curing of dental composites remains a major concern. The polymerization shrinkage in a cavity can generate stresses within the material and the tooth structure. This stress may result in cuspal deflection, enamel microcracking, interfacial debonding, postoperative sensitivity, marginal discoloration, and secondary caries. The magnitude of the polymerization stress depends on the properties of the composite and clinical

application factors, all of which can affect the degree and rate of polymerization.[1,2]

Various clinical restorative techniques, such as incremental layering,[3] the use of low-modulus liners,[4] and the control of curing-light intensity[5] have been proposed to reduce shrinkage stress. Recently, a composite containing silorane instead of methacrylate resin matrix has been introduced for that purpose. [6,7] However, concerns remain, and the measurement of shrinkage stress and its effect on marginal integrity continues to be studied aggressively.

The methods to measurement of polymerization shrinkage stress include the tensometer,[8] photoelastic analysis,[9] finite element analysis,[10] and the strain gage method.[11] The methods for assessment of the integrity of the bond between the tooth and composite include the micro-tensile bond strength test,[12] scanning electron microscopy (SEM),[13] and dye penetration.[14] However, these methods are all destructive and evaluate only the outcome at the end of polymerization. Recently, non-destructive methods, such as micro-computed tomography (micro-CT),[15] have been introduced. However, because of its lower resolution, this method cannot detect debonding at a submicron level.[16] Further, none of these methods can be used to monitor debonding during composite curing in real time.

Acoustic emission (AE) is characterized by elastic waves produced when minor damage, such as microcracks and plastic deformation, is generated in a material by internal or external stress. The AE test is a non-destructive technique

in which elastic waves propagate to the surface and are recorded by sensors coupled to the surface of the material.[17,18] The versatile AE test has many industrial applications, such as assessing structural integrity or detecting flaws, and is used extensively as a research and quality control tool due to its high sensitivity and ability to provide real-time data at the moment fracture or damage occurs. In dentistry, it has been used to monitor the fracture of particulate and fiber-reinforced composite as well as ceramics.[19-21] Recently, AE was used to monitor debonding at the tooth-composite interface,[16,22] showing a clear relationship between the number of AE events and interfacial debonding, as well as the effects of composite properties and cavity geometry on the AE characteristics. To date, however, no research has reported on AE characteristics affected by different adhesives and light-curing protocols.

The objective of this study was to use the AE technique to detect interfacial debonding at the tooth-composite interface during composite curing, and to investigate the effects of adhesive systems, light-curing methods, and composite properties on AE characteristics. The hypothesis to be tested was that composite-adhesive combinations that generate high contraction stress would be associated with a greater number of AE events and more evidence of interfacial failure during light-curing.

II. MATERIALS & METHODS

1. Materials

A methacrylate-based universal hybrid composite (Filtek Z250), a flowable composite (Filtek Z350 XT flowable), and a silorane-based composite (Filtek P90) were investigated. Two etch-and-rinse adhesives (Scotchbond Multipurpose and Single Bond 2), Two self-etch adhesives (Clearfil SE Bond and Easy Bond), and P90 System Adhesive were also used. The components, application protocols, and manufacturers of the materials are listed in Table 1.

2. Polymerization shrinkage of composites

The shrinkage of the composites was measured by a technique based on Archimedes' principle, as previously reported [23] (Figure 1). A 40-80 mg composite sample was placed on the 4 mm diameter aluminum sample pan and loaded on the arm of the balance set to the null position. After acquiring a baseline for 30 sec, the composite was exposed to the curing light (VIP, Bisco Inc., Schaunmburg, IL, USA) for 40 sec with the irradiance on the sample surface being 600 mW/cm^2. The output voltage was recorded at a sampling rate of 33 data points/s for 10 min in order to measure the buoyancy change over time, which was then converted to a volume change. The temperature of the distilled water was set to 25 ± 0.5℃. The initial sample volume was calculated from the sample weight and the density of the uncured composite measured before using a

pycnometer. This method allows for total shrinkage (%), shrinkage rate (% s^{-1}) and time to peak shrinkage rate (s) to be determined (n = 5).

3. Flexural modulus of composites

Bar type specimens (2×2×25 mm) were prepared in a stainless steel mold and light cured in 3 overlapping sections for 40 sec each at 600 mW/cm^2 (Elipar Freelight 2, 3M ESPE, St. Paul, MN, USA) (n = 5). The flexural modulus was obtained in three point bending on a universal testing machine (LF-plus, Ametek Inc., Largo, FL., USA) at a load rate of 0.5 mm/min.[24] The flexural modulus of elasticity was calculated from the equation: $E = \frac{L^3 P}{4WT^3 D}$, where E is the flexural elastic modulus (Pa), L is the support span (m), P is the load (N), W is the specimen width (m), T is the specimen thickness (m), and D is the displacement at the center of the beam (m).

4. Polymerization shrinkage stress of composites

We used the strain gage method[11] to measure shrinkage stress (Figure 2). A brass ring (inner diameter, 7 mm; outer diameter, 8 mm; height, 2 mm) was prepared. After the inner surface of the ring was sandblasted with 50 ㎛ Al_2O_3 powder, a dental adhesive was applied: Scotchbond Multipurpose adhesive was used for Z250 and Z350 XT flowable, while P90 System Adhesive was used for P90.

Polymerization shrinkage stress (σ_{ss}) of composite cured inside a brass ring was calculated as follows: $\sigma_{ss} = -E\varepsilon \frac{r_o^2 - r_i^2}{2r_i^2}$ (E, elastic modulus of brass; ε, strain; r_o, outer diameter; r_i, inner diameter)[25] (n = 5).

5. Acoustic emission (AE) test

5.1. Specimen preparation

Forty-nine extracted upper premolars were stored in 0.5% chloramine-T solution. The study was approved by the Institutional Review Board of Seoul National University Dental Hospital (CRI12001). The roots were horizontally resected at 5 mm below the cemento-enamel junction and class I cavities (bucco-lingual width, 3 mm; mesio-distal length, 4 mm; depth, 2 mm) were prepared. A 2-mm-diameter hole was made through the root in a mesio-distal direction so that the tooth could be attached to a slide glass with an elastic rubber band. Grease was applied between the tooth and the slide glass (Figure 3). The teeth were divided into 7 groups. The adhesives were applied following manufacturer's instructions, and composites were placed into the cavities in bulk.

Z250_SBMP: Cavities were acid-etched, rinsed and dried. Scotchbond Multipurpose was applied and light-cured for 10 sec. Z250 was filled and light-cured for 40 sec.

Z250_SB: Cavities were acid-etched, rinsed and dried. Single Bond 2 was

applied and light-cured for 10 sec. Z250 was filled and light-cured for 40 sec.

Z250_CFSE: Clearfil SE Bond was applied and light-cured for 10 sec. Z250 was filled and light-cured for 40 sec.

Z250_EB: Easy Bond was applied and light-cured for 10 sec. Z250 was filled and light-cured for 40 sec.

P90: P90 System Adhesive was applied and light-cured for 10 sec. P90 was filled and light-cured for 40 sec.

Z350_SBMP: Cavities were acid-etched, rinsed and dried. Scotchbond Multipurpose was applied and light-cured for 10 sec. Z350 XT flowable was filled and light-cured for 40 sec.

Z250_Exp: Cavities were acid-etched, rinsed and dried. Scotchbond Multipurpose was applied and light-cured for 10 sec. Z250 was filled and light-cured by an "exponential mode", in which the light intensity increased exponentially during the initial 5 sec, thereafter being cured with full intensity for 40 sec.

5.2. Acoustic emission (AE) during composite curing

An AE sensor (M204A, Rectuson, Sungnam, Korea) was applied with grease to the glass slide holding the tooth and located 1 cm apart (Figure 3). The AE sensor was attached to the glass, which served as a conductor of the AE signal, rather than to the tooth surface, to avoid the generation of false-positive signals that

may result from the detachment of the sensor from the external surface of the tooth during the experiment. After the tooth was filled and a 20-second baseline was obtained, the specimen was light-cured for 40 sec at 600 mW/cm^2 with an Elipar Freelight 2 (3M ESPE). After being light-cured, the outer surface of the tooth was covered with wet gauze to avoid dehydration cracking.

The signals from the AE sensor were amplified (2,500X) and stored on a computer equipped with a data acquisition board (USB-6361, National instrument, Austin, TX, USA). The measurement parameters were: sampling rate, 2 MHz; duration, 2 ms; and threshold, 70 mV. AE signals were measured for 2,000 sec after the initiation of light-curing. AE data were analyzed with AE parameters such as event number, event time and amplitude.

6. Examination of the tooth-composite interface

After the AE test, teeth were sectioned longitudinally in a bucco-lingual direction by means of a diamond saw (Isomet, Buehler, Chicago, IL, USA) to produce two 1-mm-thick specimens for each tooth. The sectioned surfaces were polished with a 1,200-grit polishing paper and acid-etched for 15 sec to remove the smear layer. Vinyl polysiloxane impressions (Examixfine, GC, Japan) were made of the sectioned surfaces, and epoxy replicas were made. The replicas were coated with Au-Pd and the tooth-composite interface was examined in a SEM (S-4700, Hitachi, Tokyo, Japan).

7. Statistical analysis

The data were analyzed by one-way ANOVA and Tukey's *post hoc* test ($\alpha = 0.05$) using SPSS version 19 (SPSS Inc.,Chicago, IL,USA).

III.RESULTS

1. Polymerization shrinkage of composites

The time dependent curves for volumetric shrinkage of the three composites for 10 min are presented in Figure 4. The shrinkage at 10 min of P90, Z250, and Z350 XT flowable was 1.65 ± 0.15%, 2.15 ± 0.13%, and 3.95 ± 0.06% respectively (Table 2 and Figure 4).

The rates of polymerization shrinkage as a function of time, which were obtained from the derivative of the shrinkage curve, are presented in Figure 5. The peak shrinkage rate of P90 was the lowest ($0.12\%s^{-1}$), followed by Z250 ($0.24\%s^{-1}$) and Z350 XT flowable ($0.45\%s^{-1}$). The peak times, an indicator of curing speed, were 6.01 sec for P90, 2.84 sec for Z250, and 3.37 sec for Z350 XT flowable (Table 2).

2. Flexural modulus of composites

The flexural moduli of P90, Z250, and Z350 XT flowable were 7.65 ± 0.22 GPa, 9.43 ± 0.58 GPa, and 5.11 ± 0.53 GPa, respectively (Table 2).

3. Polymerization shrinkage stress of composites

The shrinkage stress for all composites rapidly increased after a transient expansion, reaching a plateau after about 300 sec (Figure 6). The shrinkage stress of P90 (8.12 ± 0.37 MPa) was lower than that of Z250 (9.09 ± 0.27 MPa) and

Z350 XT flowable (11.25 ± 0.35 MPa) ($p < 0.05$). The times to reach 1 MPa of shrinkage stress were 48.1 sec for P90, 17.1 sec for Z250, and 19.6 sec for Z350 XT flowable (Table 3).

4. Acoustic emission (AE) during composite curing

A representative AE is shown in Figure 7. The duration of the signal was nearly 1 ms and the peak amplitude was 0.45 V (2,500 X).

Most AE signals of each group were weak with amplitude less than 1 V, while in Z250_CFSE and Z250_EB, strong signals higher than 4.0 V were additionally detected (Figure 8).

The mean numbers of AE events recorded were, from lowest to highest: P90 = 1.57 ± 1.51, Z250_Exp = 3.42 ± 1.99, Z250_SBMP = 3.71 ± 2.12, Z250_CFSE = 4.57 ± 2.23, Z250_SB = 4.71 ± 3.45, Z250_EB = 6.14 ± 1.86, and Z350_SBMP = 8.57 ± 4.76. The mean AE number of Z350_SBMP was greater than that of Z250_SBMP, P90, and Z250_Exp ($p = 0.022$, $p < 0.001$, $p = 0.009$, respectively). P90 showed significantly lower mean AE events than Z250_EB and Z350_SBMP ($p = 0.022$, $p < 0.001$) (Table 4 and Figure 9a). The total cumulative number of AE events of all specimens (n = 7) in each group, from lowest to highest, was: P90 = 11, Z250_Exp = 24, Z250_SBMP = 26, Z250_CFSE = 32, Z250_SB = 33, Z250_EB = 43, and Z350_SBMP = 60 (Table 4).

AE events and total cumulative AE events of groups as a function of time are presented in Figure 10. The total cumulative AE events rapidly increased at the initial stage and the rate of increase declined with time. In Z250_CFSE and Z250_EB, a high number of AE events was detected, especially within the initial 20 sec (Figures 8 and 9b). In P90, AE events were initiated 40 sec after light exposure began, while in Z350_SBMP, a high number of AE events was detected continuously, beginning immediately after the initiation of light-curing (Figure 8). Z250_Exp showed fewer AE events at the initial stage of curing compared with Z250_SBMP ($p = 0.017$) (Figure 9b).

5. SEM images of the tooth-composite interface

All the groups showed tight enamel-composite bonding (Figure 11a), except Z250_EB (Figure 11b). However, there were many gaps at the dentin-composite interface, mainly at the pulpal floor of the cavity. Z350_SBMP showed wider gaps at the dentin-composite interface compared with the other groups (Figure 11c), while P90 showed narrower gaps (Figure 11d).

IV.DISCUSSION

The polymerization shrinkage stress of dental composites has been reported to range between 3.3-23.5 MPa.[2] For successful dentin bonding, bond strength between the dental adhesive and the cavity wall should be higher than the shrinkage stress. As the composite polymerizes, the elastic modulus increases to a level that does not allow enough plastic deformation to compensate for the polymerization shrinkage.[26] Therefore, in areas where the shrinkage stress is higher than the bond strength, detectable acoustic waves can be generated at the very moment when interfacial debonding occurs. Preliminary studies up to 6 hrs showed that most AE events were generated within 20 min. Thus, the measurement time of this study was limited to 2,000 sec.

P90 exhibited the lowest shrinkage (rate), and the longest peak time, consistent with results of other studies.[6,7] The reduced shrinkage and cure rate of P90 resulted in the lowest shrinkage stress of the three composites, despite the fact that P90 had intermediate flexure modulus. It is likely that the reduced shrinkage rate allows the growing polymer chain to relieve shrinkage stress by plastic flow.

The mean AE number for P90 was lower than that of Z250_SBMP and Z350_SBMP, and two P90 specimens produced no detectable AE events. This result corresponds to the SEM analysis in which P90 showed narrower gaps at the dentin-composite interface than the other groups (Figure 11). In addition, the

first AE event of P90 was generated at 40 sec after light exposure began (Figures 8 and 9b), which coincided with the slower polymerization rate and the longest time to reach 1 MPa of shrinkage stress (Tables 2 and 3, Figures 5 and 6). In contrast, Z350 XT flowable, which had the most shrinkage and highest shrinkage rate, produced the highest shrinkage stress and generated the greatest number of AE events, which occurred continuously, beginning immediately after light-curing began (Figures 8-10). In conjunction with the interfacial SEM analysis showing the greatest debonding at the dentin-composite interface (Figure 11c), the results indicate that the AE events detected in this study were induced by debonding at the tooth-composite interface generated by the polymerization shrinkage stress of the composites. The fact that the total cumulative AE events curves (Figure 10) are similar to the shrinkage stress curves would support these results.

The exponential curing method, in which the light intensity is slowly increased during curing, was designed to slow the curing rate. Although no statistical difference was found in the mean numbers of AE events for Z250_SBMP and Z250_Exp, there was a difference in distribution, in that AE events were concentrated at the initial stage in Z250_SBMP, while Z250_Exp showed lower initial AE events (Figures 8, 9b and 10). This provided some evidence that the reduction of initial curing rate by lowering the initial light intensity in Z250_Exp produced reduced stress at the initial stage, perhaps by

enhanced flow capacity through delayed gelation.[5]

The 4 adhesives in this study can be arranged in increasing order of the mean AE events as follows: Z250_SBMP, Z250_CFSE, Z250_SB, and Z250_EB. The adhesives were chosen due to differences in bond strengths as reported in previous studies,[27,28] and though there were no significant differences in AE number, the AE pattern graphs (Figures 8 and 10) and SEM analysis agree with previously reported bond strength results. In Z250_SBMP and Z250_SB, both involving etch-and-rinse adhesives, AE events were generated over a long time, i.e., beyond 1,200 sec., While, in Z250_CFSE and Z250_EB, involving self-etch adhesives, all AE events were generated before 500 sec, and a high number of AE events was detected within the initial 20 sec (Figures 8, 9b and 10). It could be inferred that, with the etch-and-rinse adhesives (SBMP and SB), the relatively high expected bond strength resulted in good initial adhesion, followed by gradual interfacial debonding. In contrast, analysis of the AE data suggests that with the self-etch adhesives (CFSE and EB), interfacial debonding rapidly developed at the initial stages of curing, resulting in the relief of the shrinkage stress at the tooth-dentin interface after 500 sec, with few further events recorded. In addition, in Z250_CFSE and Z250_EB, strong signals with high amplitude were detected among the weak signals (Figure 8c and d), indicating that severe detachments at the interface were generated. In the SEM images, when compared with other groups showing tight enamel-composite bonding, only Z250_EB

showed the gap at the enamel-composite interface (Figure 11a and b).

The AE method could detect the debonding in real time; however, it could not identify where the debonding occurred, i.e., enamel or dentin, and in which portions of cavity walls, because the tooth-specimen size was too small for multiple sensors to be adopted.

Further investigations would be needed to investigate the effects on AE characteristics of clinical factors such as the class of cavity, cavity geometry, incremental layering, and the use of a liner, as well as other material factors such as concentration of photoinitiator, which can influence the polymerization shrinkage kinetics.

V. CONCLUSION

Within the limitations of this study, composites with lower shrinkage and slower polymerization reactions, which resulted in lower shrinkage stress, demonstrated fewer AE events, representative of fewer interfacial debonds, during cavity restoration. Different adhesive systems showed different AE generation patterns, with a trend toward fewer events with stronger adhesives. The AE test is an effective technique for monitoring the debonding kinetics at the tooth-composite interface during *in vitro* composite restoration in real time.

VI.REFERENCES

1. Braga RR, Ballester RY, Ferracane JL. Factors involved in the development of polymerization shrinkage stress in resin-composites: A systematic review. Dent Mater 2005;21:962-970.

2. Kleverlaan CJ, Feilzer AJ. Polymerization shrinkage and contraction stress of dental resin composites. Dent Mater 2005;21:1150-1157.

3. Park JK, Chang JH, Lee IB. How should composite be layered to reduce shrinkage stress: Incremental or Bulk filling? Dent Mater 2008;24:1501-1505.

4. Braga RR, Ferracane JL. Alternatives in polymerization contraction stress management. Crit Rev Oral Biol Med 2004;15:176-184.

5. Obici AC, Sinhoreti MAC. De Goes MF. Consai S, Sobrinho LC. Effect of the photo-activation method on polymerization shrinkage of restorative composites. Oper Dent 2002;27:192-198.

6. Weinmann W, Thalacker C, Guggenberg R. Siloranes in dental composites. Dent Mater 2005;21:68-74.

7. Papadogiannis D, Kakaboura A. Palaghias G, Eliades G. Setting characteristic and cavity adaptation of low-shrinkage resin composites. Dent Mater 2009;25:1509-1516.

8. Lee SH, Chang J, Ferracane J, Lee IB. Influence of instrument compliance and specimen thickness on the polymerization shrinkage stress measurement of light-cured composites. Dental Mater 2007;23:1093-1100.

9. Kinomoto Y, Torii M, Takeshige F. Polymerization contraction stress of resin composite restorations in a model class I cavity configuration using photo elastic analysis. J Esthet Dent 2000;12:309-319.

10. Ausiello P, Apicella A, Davidson CL. Effect of adhesive layer properties on

stress distribution in composite restorations – a 3D finite element analysis. Dent Mater 2002;18:295-303.

11. Sakaguchi RL, Peters MC, Nelson SR, Douglas WH, Poort HW. Effect of polymerization contraction in composite restorations. J Dent 1992;20:178-182.

12. Takemori T, Chigira H, Itoh K, Hisamitsu H. Factors affecting tensile bond strength of composite to dentin. Dent Mater 1993;9:136-138.

13. Ciucchi B, Bouillaguet S, Delaloye M, Holz J. Volume of the internal gap formed under composite restorations in vitro. J Dent 1997;25:305-312.

14. Leevailoj C, Cochran MA, Matis BA, Moore BK, Platt JA. Microleakage of posterior packable resin composites with and without flowable liners. Oper Dent 2001;26:302-307.

15. De Santis R, Mollica F, Prisco D, Rengo S, Ambrosio L, Nicolais L. A 3D anaylsis of mechanically stressed dentin-adhesive-composite interface using X-ray micro-CT. Biomaterials 2005;26:257-270.

16. Li H, Li j, Yun X, Liu X, Fok ASL. Non-destructive examination of interfacial debonding using acoustic emission. Dent Mater 2011;27:964-971.

17. Hamstad MA. A review: Acoustic emission, a tool for composite-materials studies. Experimental mechanics 1986;26:7-13.

18. Lee JO, Gee HS, Ju NH. Principles and applications of acoustic emission (AE) test. Mechanics & Materials 2009;21:156-164.

19. Kim KH, Okuno O. Microfracture behaviour of composite resins containing irregular-shaped fillers. J Oral Rehabil 2002;29:1153-1159.

20. Alander P, Lassila LVJ Tezvergil A, Vallittu PK. Acoustic emission analysis of fiber-reinforced composite in flexural testing. Dent Mater 2004;20:305-312.

21. Ereifej N, Silikas N, Watts DC. Initial versus final fracture of metal-free crowns, analyzed via acoustic emission. Dent Mater 2008;24:1289-1295.

22. Gu JU, Choi NS, Arakawa K. Interfacial fracture analysis of human tooth-composite resin restoration using acoustic emission. Journal of The Korea Society for Composite Materials 2009; 22:45-51.

23. Lee IB, Cho BH, Son HH, Um CM. A new method to measure the polymerization shrinkage kinetics of light cured composites. J Oral Rehabil 2005; 32: 304-314.

24. Kwon Y, Ferracane J, Lee IB. Effect of layering methods, composite type, and flowable liner on the polymerization shrinkage stress of light cured composites. Dent Mater 2011;28:801-809.

25. Riley WF, Sturges LD, Morris DH. Mechanics of Materials. 5th Ed. John Wiley & Sons Inc., New York 1999; 249-252.

26. Dauvillier BS, Feilzer AJ, de Gee AJ, Davidson CL. Viscoelastic parameters of dental restorative materials during setting. J Dent Res 2000;79:818-823.

27. De Munck J, Van Landuyt K, Peumans M, Poitevin A.Van Meerbeek B. A critical review of the durability of adhesion to tooth tissue: Methods and results. J Dent Res 2005;84:118-132.

28. Peumans M, Kanumilli P, De Menck J, Van Landuyt K, Van Meerbeek B. Clinical effectiveness of contemporary adhesives: a systematic review of current clinical trials. Dent Mater 2005;21:864-881.

Table 1. Materials used in this study

Materials (Batch No.)	Components	Application protocol	Manufacturer
Filtek Z250 (N314584)	Bis-GMA, Bis-EMA, UDMA, TEGDMA Silane treated Zr/Silica (82 wt%)	light cure: 40 sec	3M ESPE, St. Paul, MN, USA
Filtek Z350 XT flowable (N283071)	Bis-GMA, TEGDMA, YbF3 Silane treated Zr/Silica (65wt%)	light cure: 40 sec	3M ESPE
Filtek P90 (N327380)	3,4-Epoxycyclohexylcyclopolymethylsiloxane, Bis-3,4-Epoxycyclohexylethgyl-phenyl-methyl silane, Silane treated Quartz, Yttrium fluoride (76 wt%)	light cure: 40 sec	3M ESPE
Scotchbond Multipurpose (Primer: N280856 Adhesive: N244334)	Primer: Water, HEMA Adhesive: Bis-GMA, HEMA	etch: 15 sec rinse: 15 sec Primer: apply, dry: 5 sec Adhesive: apply, light cure: 10 sec	3M ESPE
Single Bond 2 (N233226)	Bis-GMA, UDMA, HEMA Ethyl alcohol, Water Silane treated silica (nanofiller) Glycerol 1, 3 dimethacrylate, Copolymer of Acrylic and Itaconic acids	etch: 15 sec rinse:10 sec Adhesive: apply, dry: 5 sec light cure: 10 sec	3M ESPE
Clearfil SE Bond (Primer: 01063A Bond: 01587A)	Self etching primer : MDP, HEMA, Water, N,N-diethanol-p-toluidine, Bond: MDP, Bis-GMA, HEMA, N,N-diethanol-p-toluidine, Silanated colloidal silica	Primer: apply: 20 sec, dry Bond: apply, light cure: 10 sec	Kuraray Medical Inc., Okayama, Japan
Easy Bond (407614)	HEMA, Bis-GMA, Ethanol, Water, Methacrylated phosphoric esters,	apply: 20 sec dry: 5 sec	3M ESPE

	1,6 hexanediol dimethacrylate, Silane treated silica	light cure: 10 sec	
P90System Adhesive (Primer: N272624 Bond: N273405)	Self etch primer: Bis-GMA, HEMA, Ethanol, Water, Phosphorylated methacrylates, Initiators, Stabilizers, Silane treated silica Bond: TEGDMA, Phosphorylated methacrylates, Initiators, Stabilizers, Silane treated silica,	Primer: apply: 15 sec, dry, light cure: 10 sec Bond: apply, dry, light cure: 10 sec	3M ESPE

Table 2. Polymerization shrinkage (%), peak shrinkage rate (%s^{-1}), peak time (s), and flexural modulus (GPa) of composites

Composites	Volume shrinkag (%)	Peak shrinkage rate (vol%s^{-1})	Peak time (s)	Flexural modulus (GPa)
Z250	2.15 (0.13)[b]	0.24	2.84	9.43 (0.58)[a]
Z350 XT flowable	3.95 (0.06)[a]	0.45	3.37	5.11 (0.53)[c]
P90	1.65 (0.15)[c]	0.12	6.01	7.65 (0.22)[b]

The numbers in parenthesis are standard deviations.

Same superscript letters in the column mean that there is no statistical difference.

Table 3. Polymerization shrinkage stress (MPa) for 2,000 sec and time (s) to reach 1 MPa of 3 composites

Composites	Polymerization shrinkage stress (MPa)	Time to reach 1 MPa (s)
Z250	9.09 (0.27)[b]	17.1
Z350 XT flowable	11.25 (0.35)[a]	19.6
P90	8.12 (0.37)[c]	48.1

The numbers in parenthesis are standard deviations.

Same superscript letters mean that there is no statistical difference.

Table 4. Mean AE events number and total cumulative AE events number of groups for 2,000 sec

Group	Mean AE events number	Total cumulative AE events number
Z250_SBMP	3.71 (2.12)^{bc}	26
Z250_SB	4.71 (3.45)^{abc}	33
Z250_CFSE	4.57 (2.23)^{abc}	32
Z250_EB	6.14 (1.86)^{ab}	43
P90	1.57 (1.51)^{c}	11
Z350_SBMP	8.57 (4.76)^{a}	60
Z250_Exp	3.43 (1.99)^{bc}	24

Total cumulative AE events number is the sum of AE events of all seven specimens in each group.

The numbers in parenthesis are standard deviations.

Same superscript letters mean that there is no statistical difference.

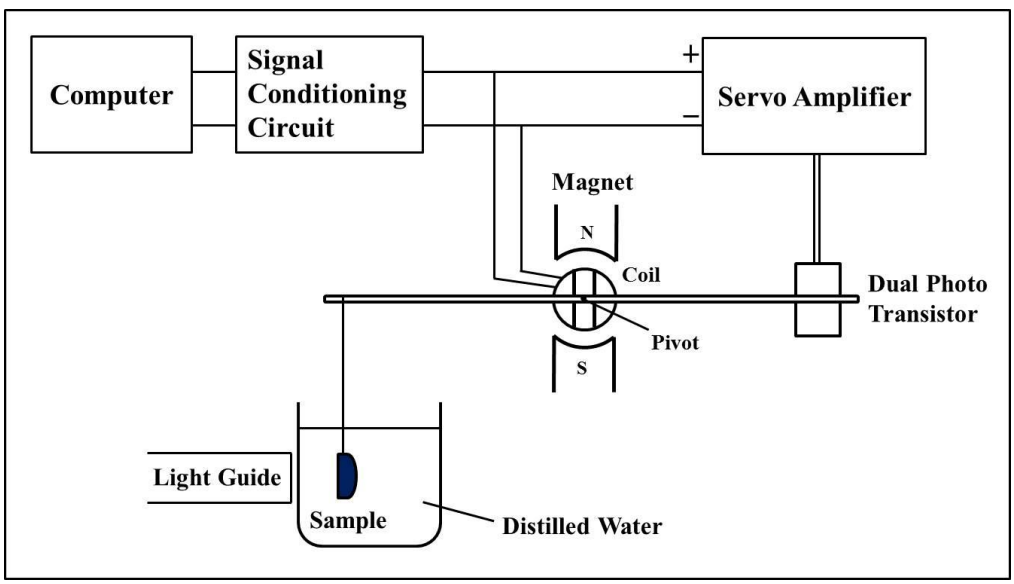

Figure 1. Schematic diagram of the instrument for measuring polymerization shrinkage.

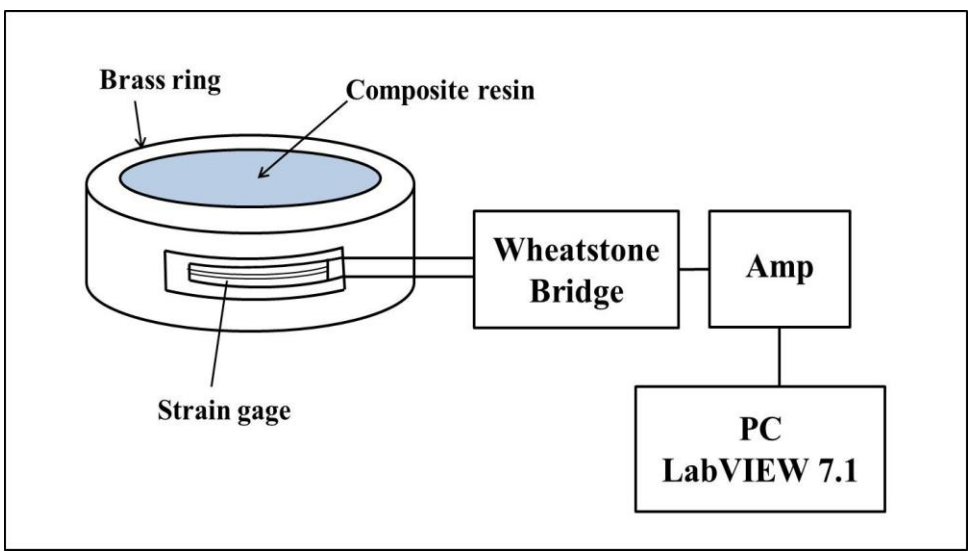

Figure 2. Schematic diagram of specimen with strain gage for measuring polymerization shrinkage stress.

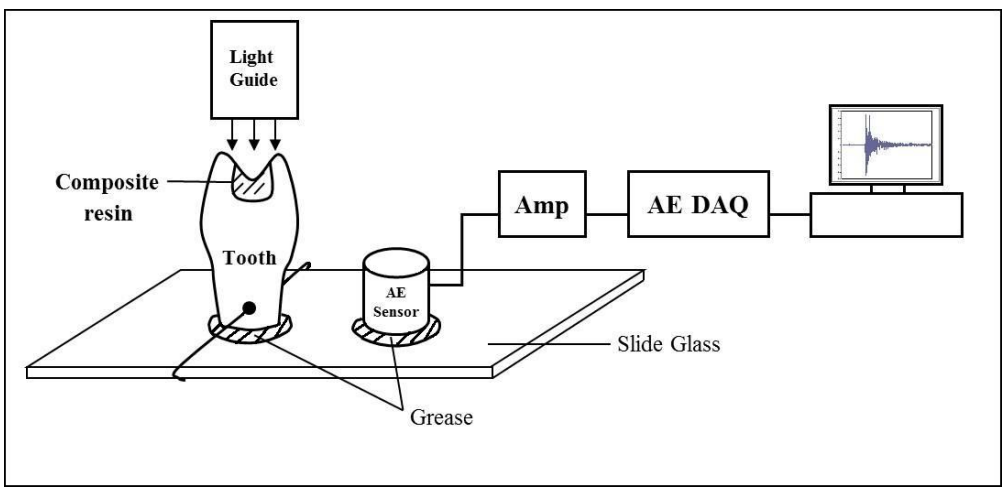

Figure 3. Schematic diagram of AE testing instrument. Polymerization shrinkage stress during light-curing of composite can cause debonding at the tooth-composite interface, which generates acoustic emission (AE) signals. The signals detected by the AE sensor, a piezoelectric ultrasonic transducer, are amplified and stored on a computer equipped with a data acquisition board (DAQ). The measurement parameters were: sampling rate, 2 MHz; duration, 2 ms; and threshold, 70 mV. AE signals were measured for 2,000 sec after the initiation of light-curing. AE data were analyzed with AE parameters such as event number, event time, and amplitude.

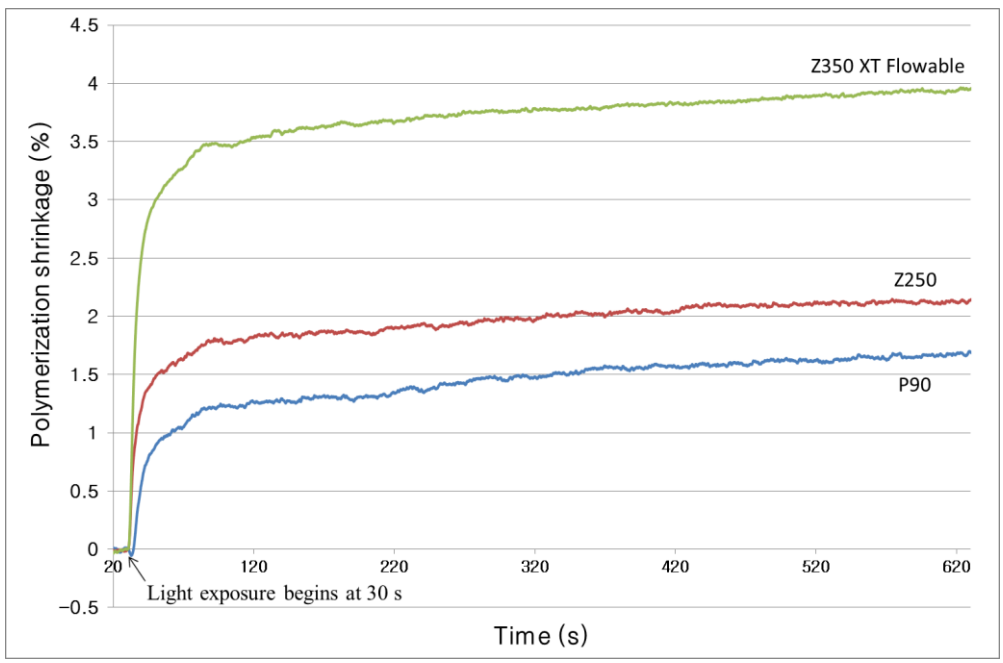

Figure 4. Representative polymerization shrinkage (%) curves vs. time (s) of 3 composites for 10 min. The shrinkage at 10 min of P90, Z250, and Z350 XT flowable was 1.65 ± 0.15%, 2.15 ± 0.13%, and 3.95 ± 0.06%, respectively.

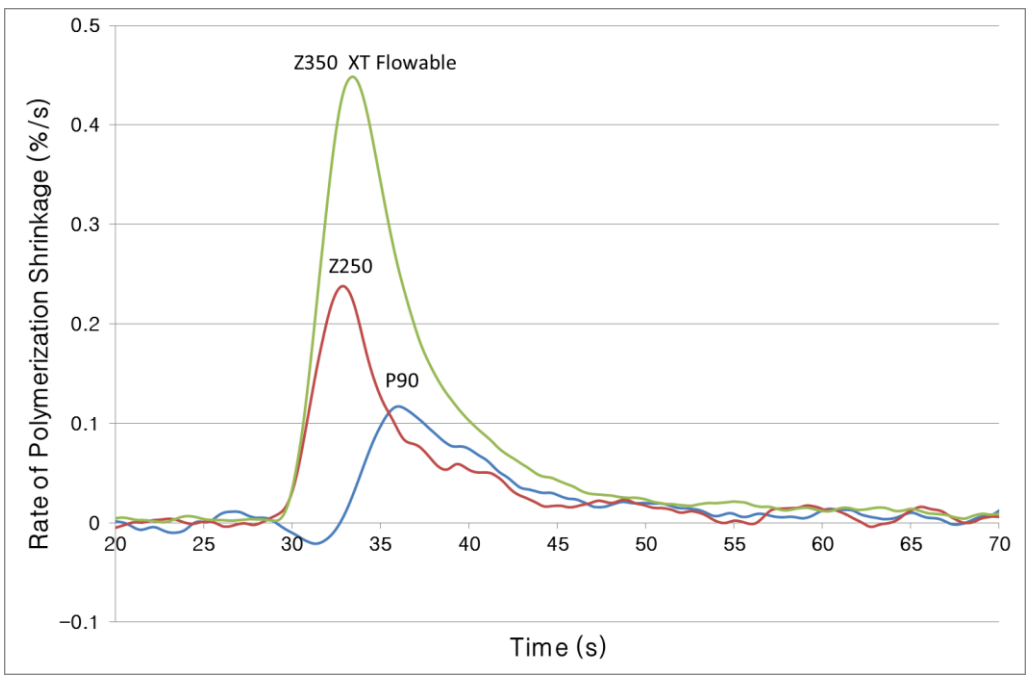

Figure 5. Polymerization shrinkage rate (%s^{-1}) curves vs. time (s) of 3 composites. The rates of polymerization shrinkage as a function of time were obtained from the derivative of the shrinkage curve. The peak shrinkage rate of P90 was the lowest (0.12%s^{-1}), followed by Z250 (0.24%s^{-1}) and Z350 XT flowable (0.45%s^{-1}).

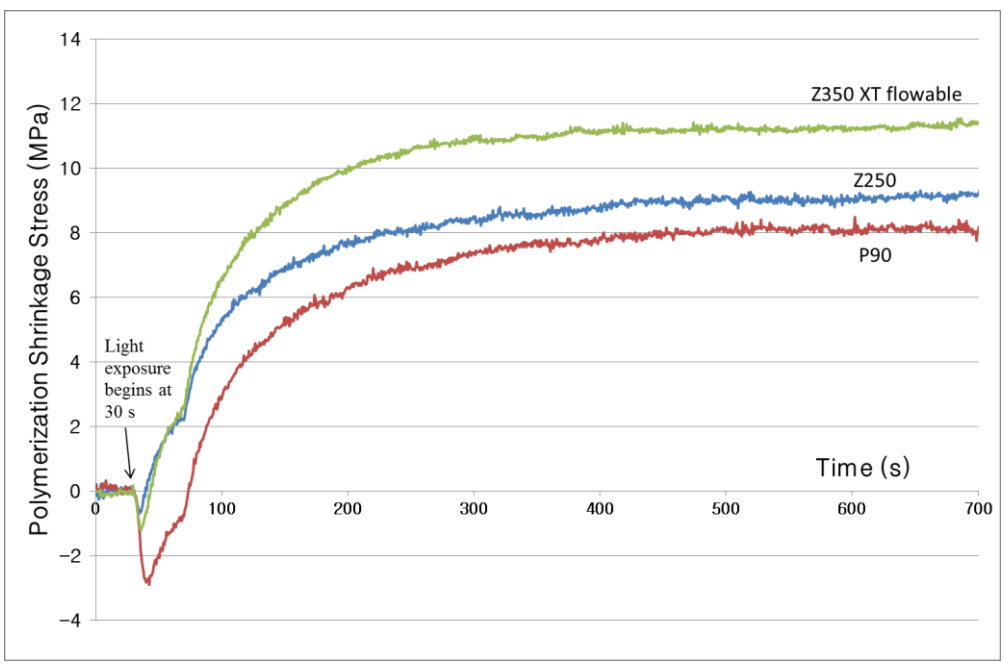

Figure 6. Change of shrinkage stress (MPa) in each group for 10 min. The shrinkage stress for all composites rapidly increased after a transient expansion, reaching a plateau after about 300 sec. The shrinkage stress of P90 (8.12 ± 0.37 MPa) was lower than that of Z250 (9.09 ± 0.27 MPa) and Z350 XT flowable (11.25 ± 0.35 MPa).

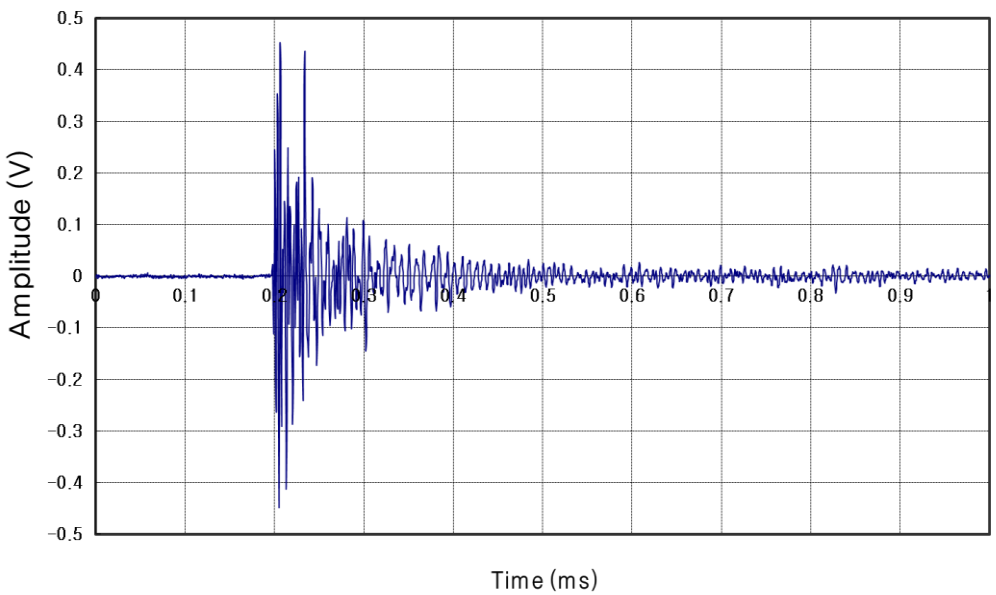

Figure 7. A representative AE signal. The measurement parameters were: sampling rate, 2 MHz; duration, 2 ms; and threshold, 70 mV. The elastic waves produced by debonding at the tooth-composite interface propagate to the surface and are recorded by a piezoelectric ultrasonic sensor. AE parameters such as event number, event time and amplitude were analyzed.

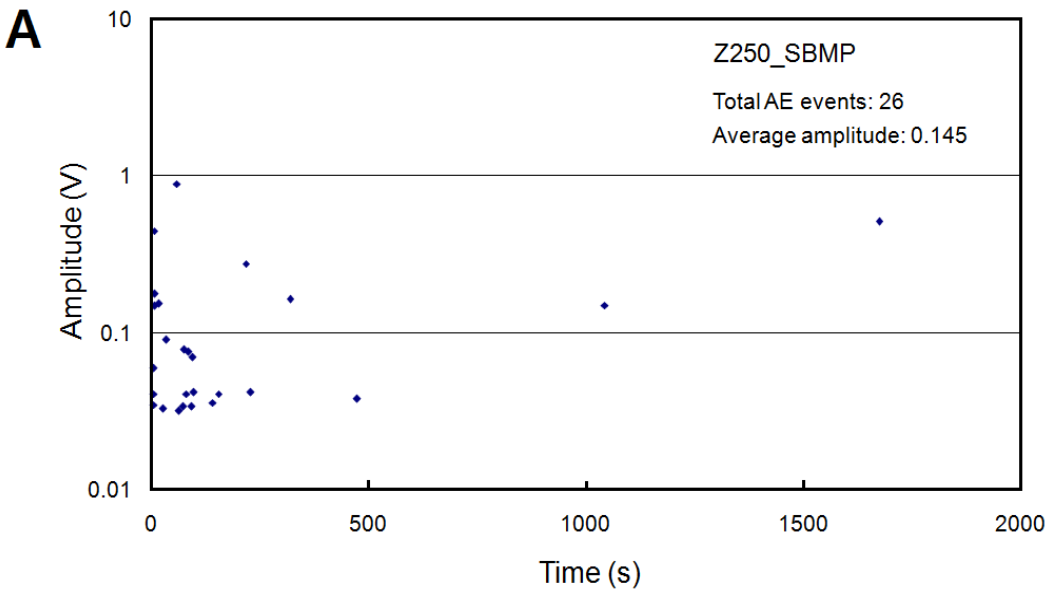
A
Z250_SBMP
Total AE events: 26
Average amplitude: 0.145
Amplitude (V)
10
1
0.1
0.01
0
500
1000
1500
2000
Time (s)

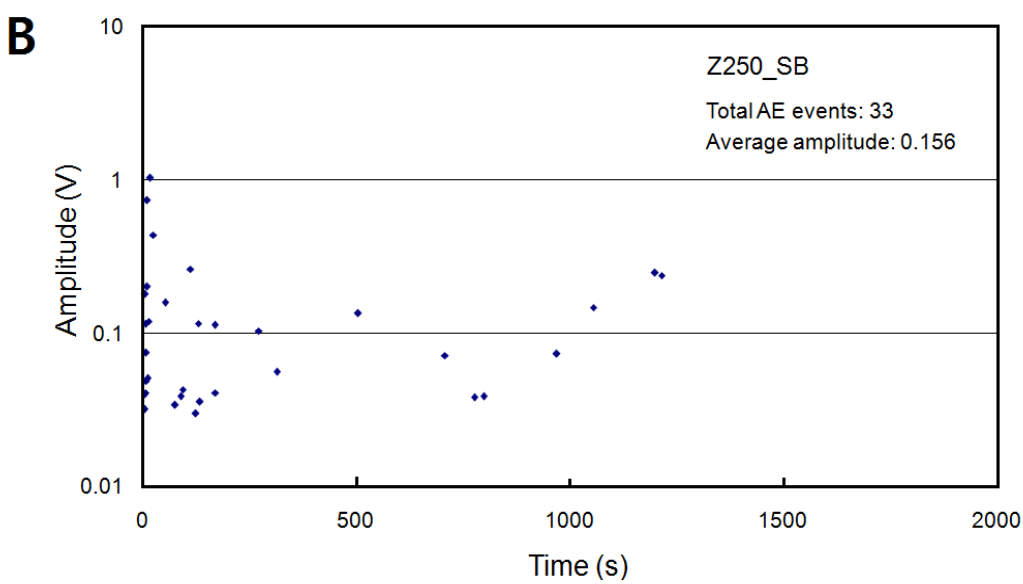
B
Z250_SB
Total AE events: 33
Average amplitude: 0.156
Amplitude (V)
10
1
0.1
0.01
0
500
1000
1500
2000
Time (s)

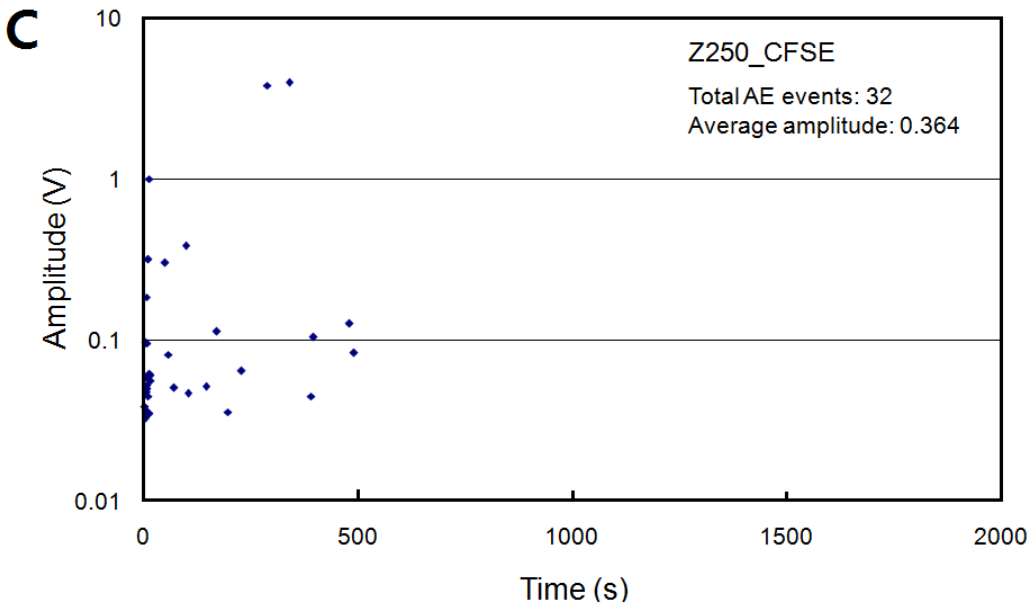
C
Z250_CFSE
Total AE events: 32
Average amplitude: 0.364
Amplitude (V)
10
1
0.1
0.01
0
500
1000
1500
2000
Time (s)

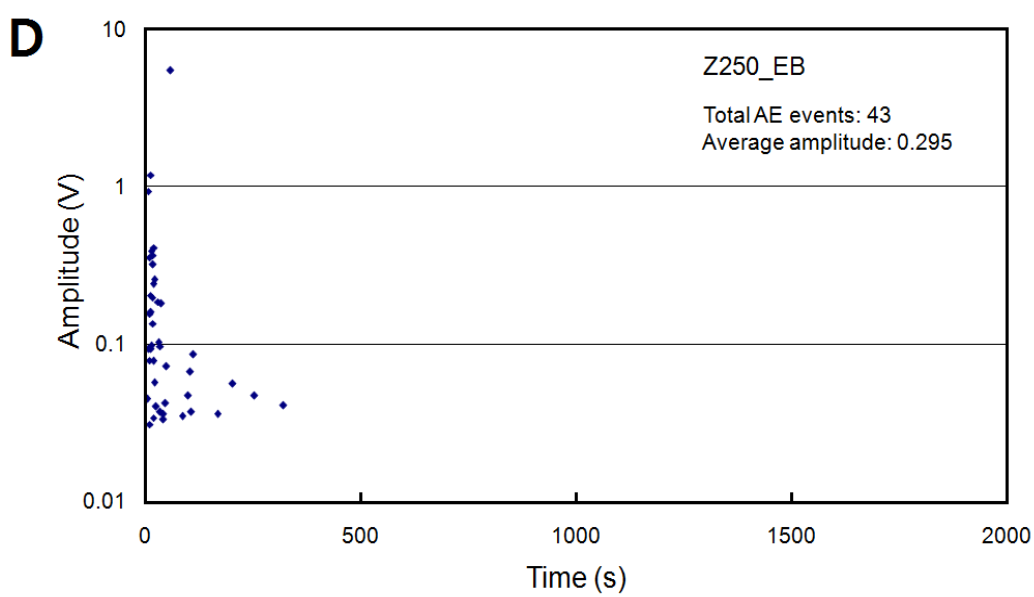
D
Z250_EB
Total AE events: 43
Average amplitude: 0.295
Amplitude (V)
10
1
0.1
0.01
0
500
1000
1500
2000
Time (s)

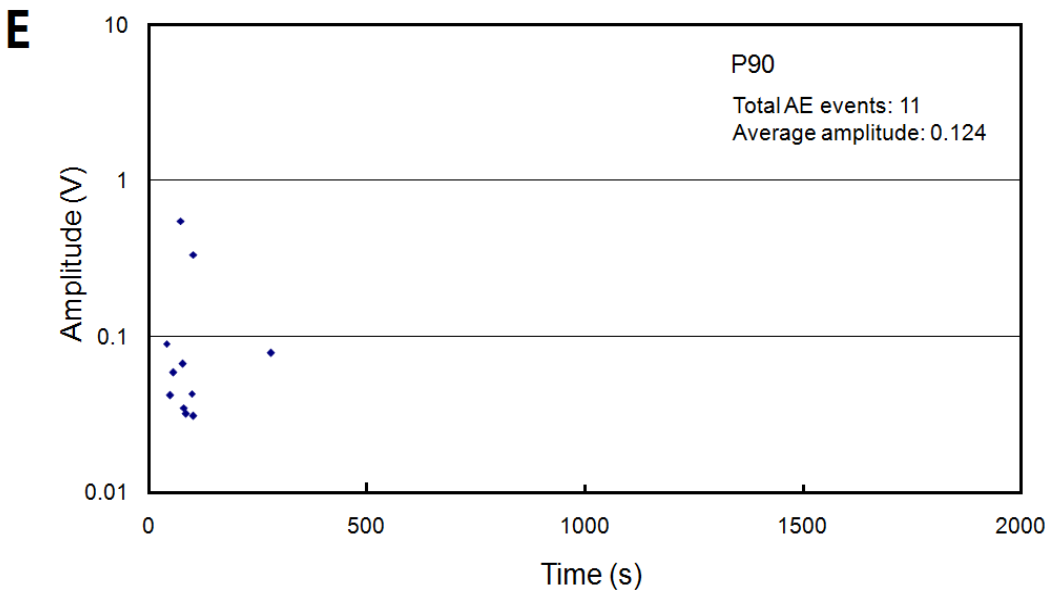
E
P90
Total AE events: 11
Average amplitude: 0.124
Amplitude (V)
10
1
0.1
0.01
0
500
1000
1500
2000
Time (s)

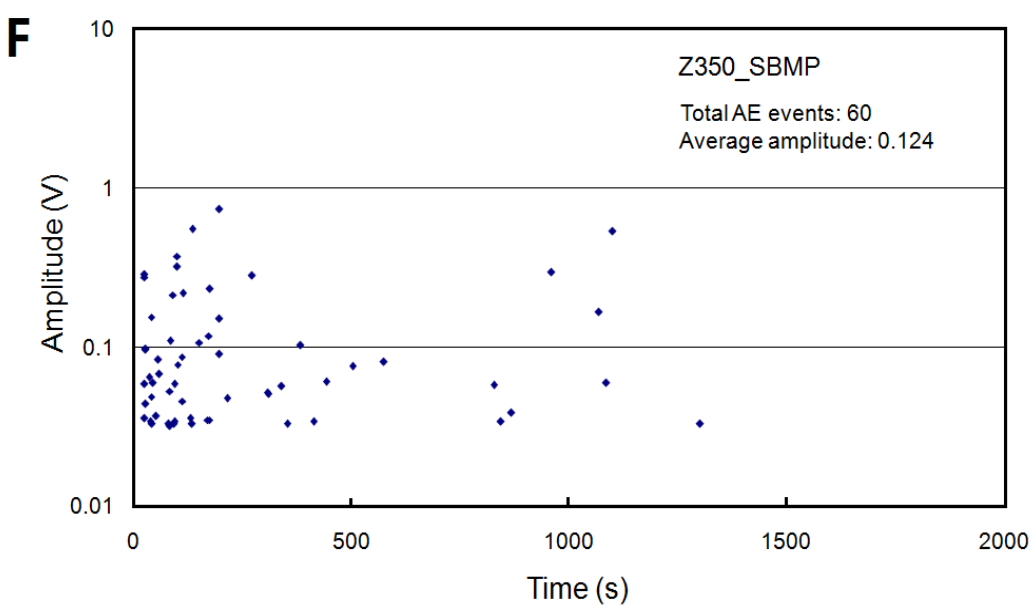
F
Z350_SBMP
Total AE events: 60
Average amplitude: 0.124
Amplitude (V)
10
1
0.1
0.01
0
500
1000
1500
2000
Time (s)

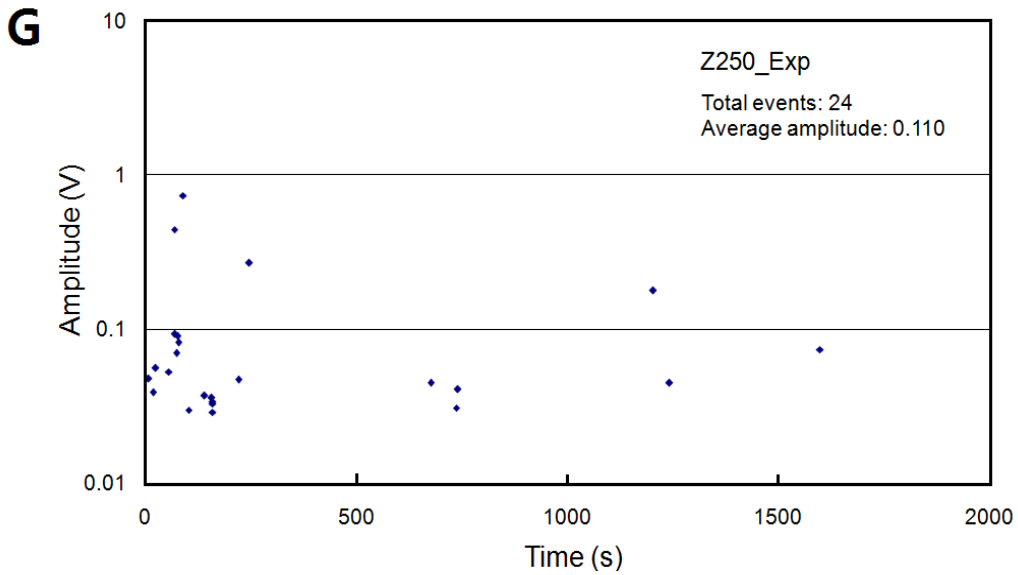

Figure 8. Total AE events and amplitude distribution of all specimens in each group (n = 7) vs. time for 2,000 sec are plotted in a graph. Each dot shows a single AE event, and the average amplitude is the mean output voltage of all AE signals in each group. (A) Z250_SBMP. (B) Z250_SB. (C) Z250_CFSE. (D) Z250_EB. (E) P90. (F) Z350_SBMP. (G) Z250_Exp.

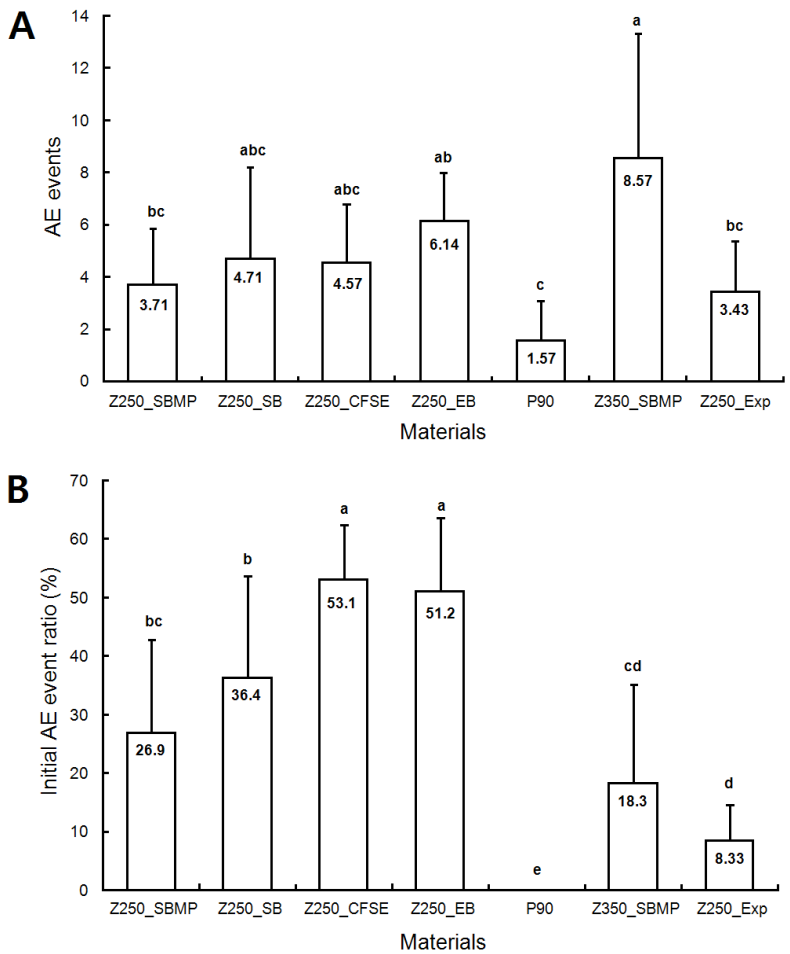

Figure 9. Mean AE event number and initial AE event ratio of each group. (A) Mean AE events per group for 2,000 sec. The mean AE number of Z350_SBMP was greater than that of Z250_SBMP, P90 and Z250_Exp. P90 showed significantly fewer mean AE events than Z250_EB and Z350_SBMP. (B) Initial AE event ratio (%) within 20 sec compared with total AE events for 2,000 sec (n = 7 specimens). In Z250_CFSE and Z250_EB, a high number of AE events was detected within the initial 20 sec. P90 specimens produced no detectable AE events within 20 sec. Z250_Exp showed fewer AE events at the initial stage of curing compared with Z250_SBMP. *Same superscript letters mean that there is no statistical difference. *Initial AE event ratio (%) = 100 × (AE events within 20 sec/Total AE events for 2,000 sec).

A

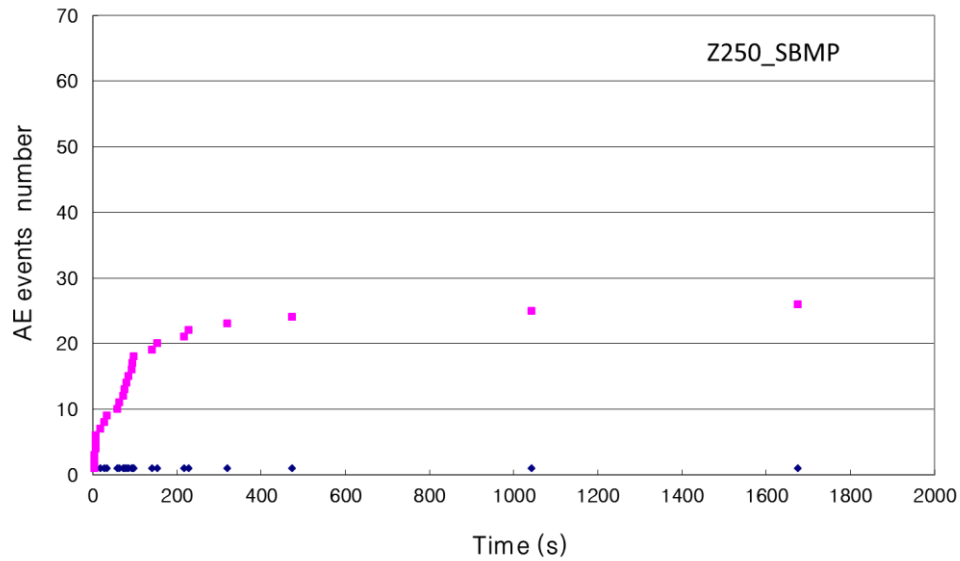
Z250_SBMP
AE events number
Time (s)
0
10
20
30
40
50
60
70
0
200
400
600
800
1000
1200
1400
1600
1800
2000

B

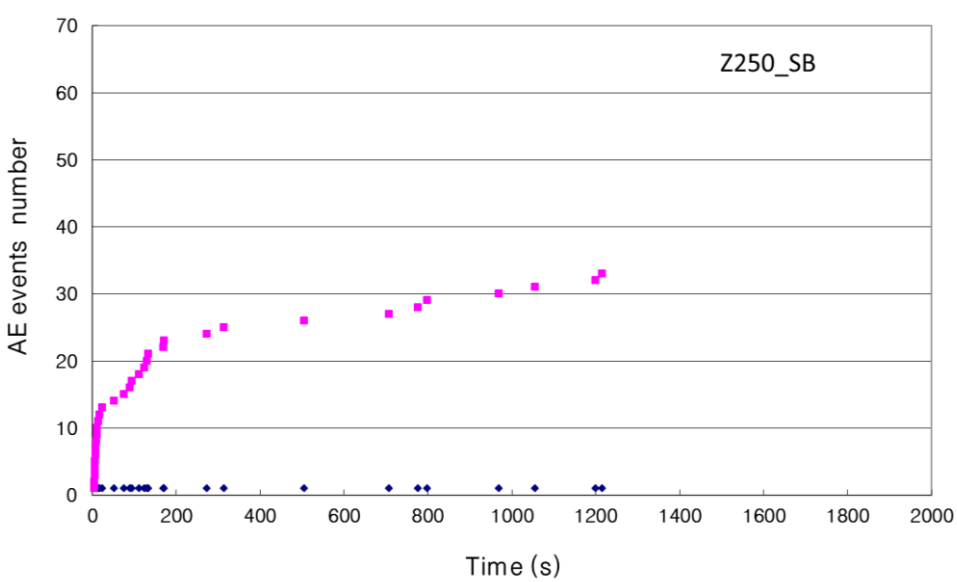
Z250_SB
AE events number
Time (s)
0
10
20
30
40
50
60
70
0
200
400
600
800
1000
1200
1400
1600
1800
2000

C

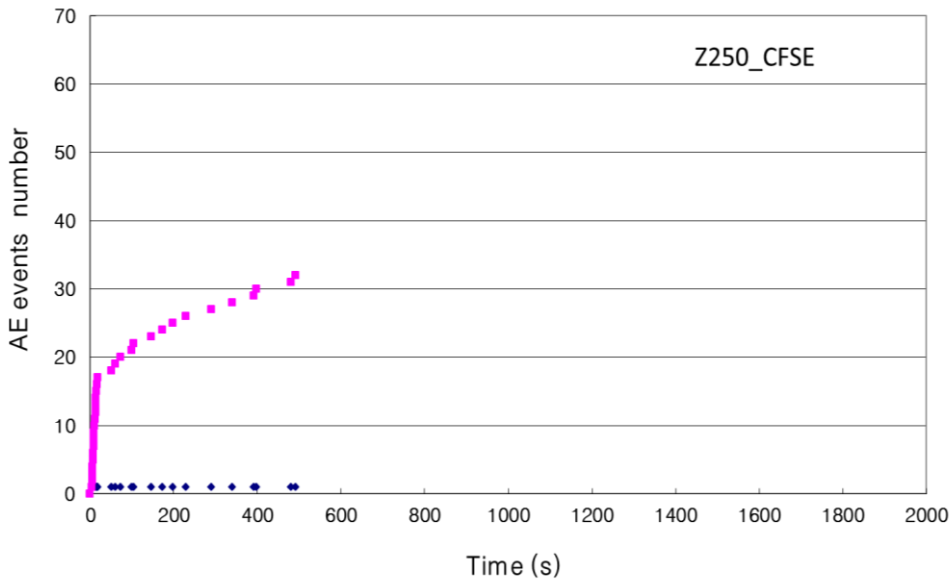
Z250_CFSE
AE events number
Time (s)
0
10
20
30
40
50
60
70
0
200
400
600
800
1000
1200
1400
1600
1800
2000

D

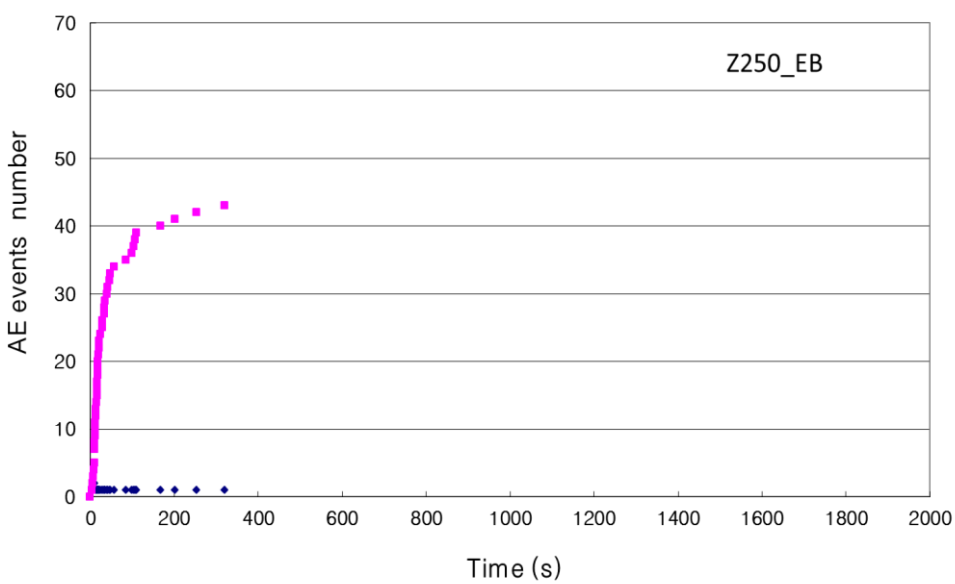
Z250_EB
AE events number
Time (s)
0
10
20
30
40
50
60
70
0
200
400
600
800
1000
1200
1400
1600
1800
2000

E

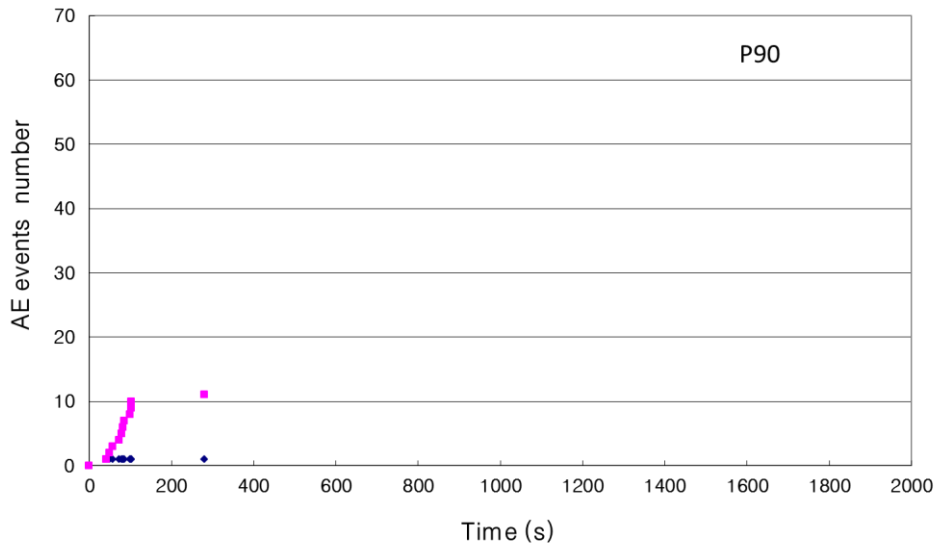
P90
AE events number
Time (s)
0
10
20
30
40
50
60
70
0
200
400
600
800
1000
1200
1400
1600
1800
2000

F

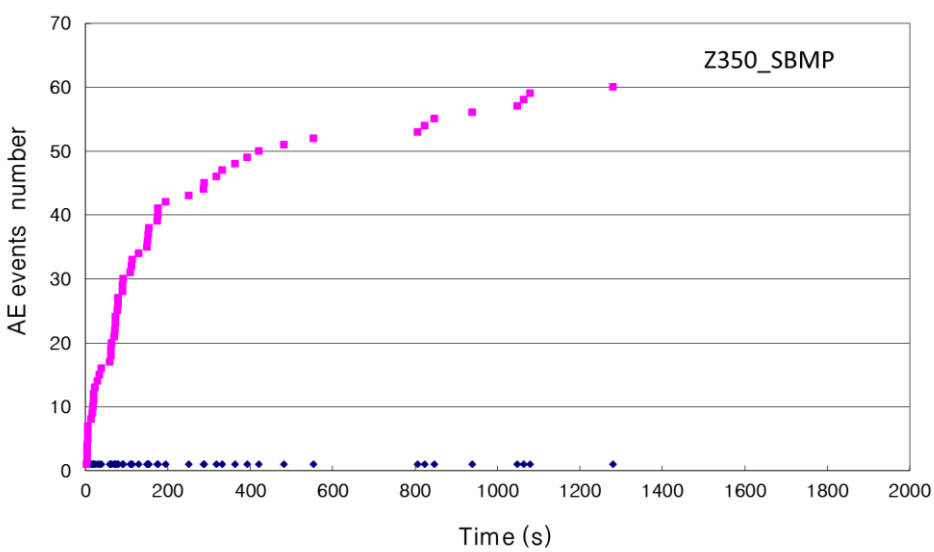
Z350_SBMP
AE events number
Time (s)
0
10
20
30
40
50
60
70
0
200
400
600
800
1000
1200
1400
1600
1800
2000

G

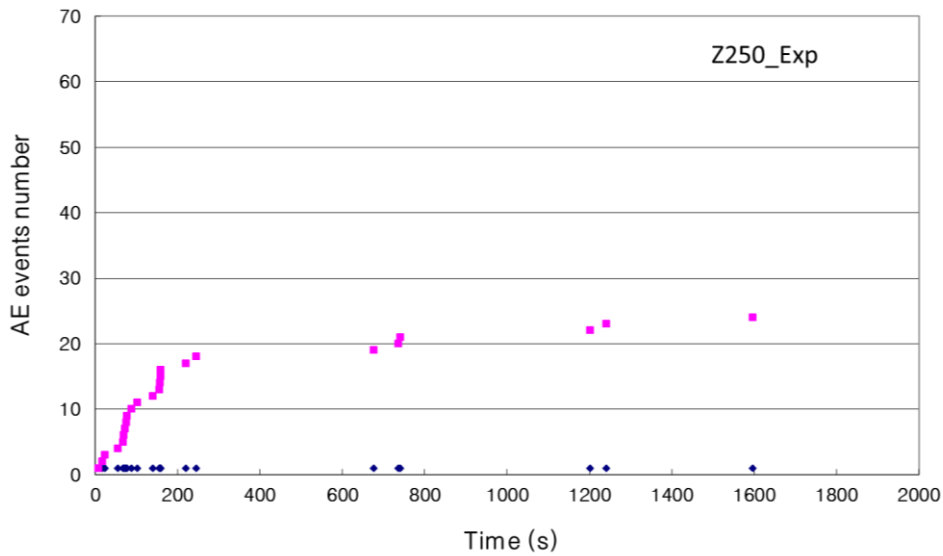

Figure 10. Total cumulative AE events of groups for 2,000 sec. The total cumulative AE events are the sum of AE events of all seven specimens in each group. (A) Z250_SBMP. (B) Z250_SB. (C) Z250_CFSE. (D) Z250_EB. (E) P90. (F) Z350_SBMP. (G) Z250_Exp.

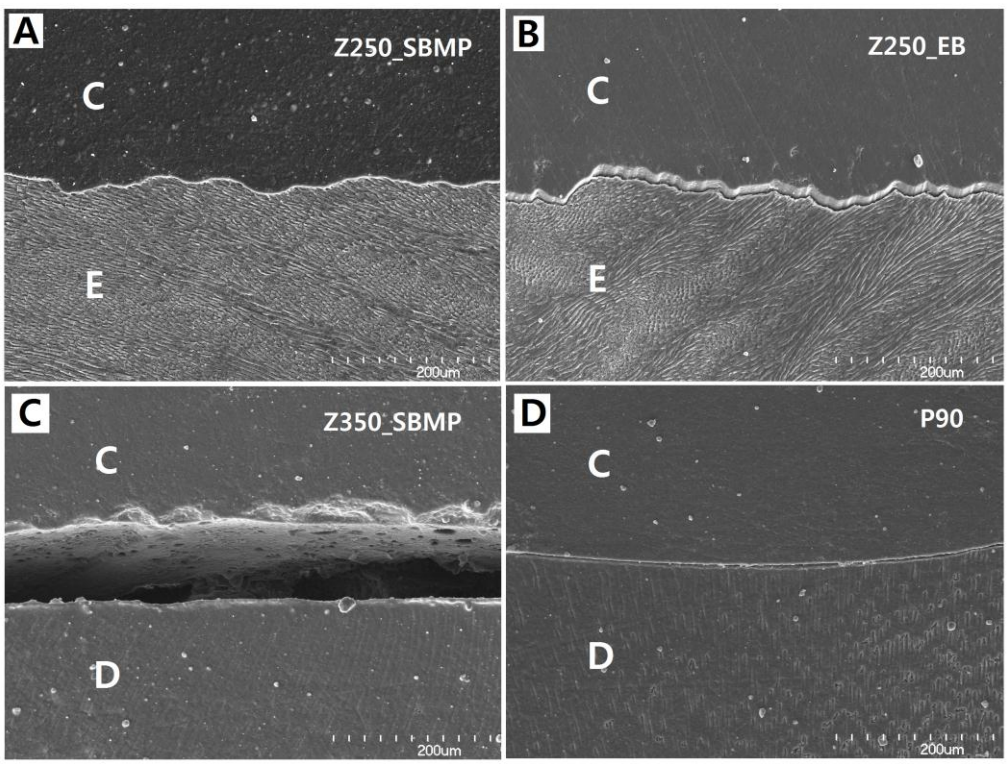

Figure 11. SEM images of the tooth-composite interface. (A) The tight enamel-composite bonding in Z250_SBMP. Z250_SB, Z250_CFSE, P90, Z350_SBMP, and Z250_Exp also showed similar patterns. (B) The gap formed between the enamel and composite in Z250_EB. (C) The wide gap formed between the dentin and composite in Z350_SBMP. (D) The narrow gap formed between the dentin and composite in P90 (C: composite, E: enamel, D: dentin).

국문초록

광중합 복합레진 수복 중 복합레진-치아 계면의 접착 파괴에 관한 음향방출분석

조 낙 연

서울대학교 대학원 치의과학과 치과보존학전공

(지도교수 이 인 복)

1. 목적

본 연구의 목적은 음향방출법을 이용하여 복합레진 수복 중 복합레진-치아 계면에서 발생하는 균열음을 실시간으로 검출하고, 복합레진과 접착제의 종류, 그리고 광중합 방법에 따른 음향방출특성의 차이를 비교하기 위함이다.

2. 재료 및 방법

Methacrylate 기질의 혼합형 복합레진, 유동성 복합레진 및 silorane 기질의 복합레진 각각의 중합수축량, 탄성계수 및 중합수축 응력을

측정하였다. 건전한 49개의 소구치에 1급 와동을 형성하고 상기 3종의 복합레진 중 하나와, 접착제로는 2종의 산부식 접착제, 2종의 자가부식 접착제 그리고 silorane 기질 레진 전용 접착제 중 하나를 이용하여 와동을 수복하였다. 복합레진-치아 계면의 균열음을 검출하기 위하여 치아가 부착된 슬라이드 글라스에 grease를 바르고 음향방출 센서를 부착하였다. 센서로부터 얻어진 신호는 증폭기를 통해 증폭된 후 컴퓨터에 저장되었다. 음향방출은 중합 개시부터 2,000초 동안 측정하였다. 음향방출 측정이 끝난 시편을 절단하여 replica를 제작하고 SEM으로 복합레진-치아 접착 계면을 관찰하였다.

3. 결과

Silorane 기질의 복합레진이 중합수축량과 최대중합수축률이 가장 낮았고 최대수축시간이 가장 느렸다. 또한 중합수축응력이 가장 낮았고 음향방출 사상수가 가장 적었다. 대부분의 복합레진-접착제 조합에서 광중합 초기에 음향방출 신호가 발생하기 시작한 것과는 대조적으로 silorane 기질의 복합레진에서는 40초 이후에 신호가 발생하기 시작하였다. 자가부식 접착제를 사용한 군은 산부식 접착제를 사용한 군과 비교하여 초기에 음향방출 사상이 집중적으로 발생하였다. 주사전자현미경 관찰 결과, 유동성 복합레진은 상아질과의 접착면에서 상당히 넓은 간극을 보인 반면, silorane 기질의

복합레진에서는 간극이 매우 좁았다.

4. 결론

중합수축이 적고 중합반응 속도가 느린 복합레진이 중합수축응력도 낮았고 음향방출 사상수도 적었다. 음향방출법은 복합레진의 수복 중 복합레진과 치아의 계면 분리를 실시간으로 검출 할 수 있는 유용한 방법이었다.

주요어: 복합레진, 복합레진-치아 계면, 음향방출, 중합수축응력, silorane

학번: 2011-30678